Observation of the Askaryan Effect

D. Saltzberg[1], P.W. Gorham[2], D. Walz[3], C. Field[3], R. Iverson[3], A. Odian[3], G. Resch[2], P. Schoessow[4], and D. Williams[1]

[1]*Department of Physics and Astronomy, University of California, Los Angeles, CA 90095*
[2]*Jet Propulsion Laboratory, Calif. Institute of Technology, Pasadena, CA, 91109*
[3]*Stanford Linear Accelerator Center, Stanford University, Stanford, CA 94309*
[4]*Argonne National Laboratory, Argonne, IL*

Abstract. We present direct experimental evidence for the charge excess in high energy particle showers and corresponding radio emission predicted nearly 40 years ago by Askaryan. We directed picosecond pulses of GeV bremsstrahlung photons at the SLAC Final Focus Test Beam into a 3.5 ton silica sand target, producing electromagnetic showers several meters long. A series of antennas spanning 0.3 to 6 GHz detected strong, sub-nanosecond radio frequency pulses produced by the showers. Measurements of the polarization, coherence, timing, field strength vs. shower depth, and field strength vs. frequency are completely consistent with predictions. We also show the emission peaks at the Cherenkov angle in sand. These measurements thus provide strong support for experiments designed to detect high energy cosmic rays such as neutrinos via coherent radio emission from their cascades in dense dielectric media.

I INTRODUCTION

During the development of a high-energy electromagnetic cascade in normal matter, Compton scattering knocks electrons from the material into the shower. In addition, positrons in the shower annihilate in flight. The combination of these processes should lead to a net 20-30% negative charge excess for the comoving compact body of particles that carry most of the shower energy. Askaryan [1] first described this effect, and noted that it should lead to strong coherent radio and microwave Cherenkov emission for showers that propagate within a dielectric. The range of wavelengths over which coherence obtains depends on the form factor of the shower bunch—wavelengths shorter than the bunch length suffer from destructive interference and coherence is lost. However, in the fully coherent regime the radiated energy scales quadratically with the net charge of the particle bunch, and hence with the incoming energy. At ultra high energies the resulting coherent radio emission may carry off a significant fraction of the total energy in the cascade.

The plausibility of Askaryan's arguments combined with more recent modeling and analysis [2–4] has led to a number of experimental searches for high energy neutrinos by exploiting the effect at energies from $\sim 10^{16}$ eV in Antarctic ice [5,6] up to 10^{20} eV or more in the lunar regolith, using large ground-based radio telescopes [7–9]. Radio frequency pulses have been observed for many years from extensive air showers [10,11]. However, it has been shown [12,13] that the dominant source of this emission is due to geomagnetic separation of charges, rather than the Askaryan effect. Thus neither the charge asymmetry nor the resulting coherent Cherenkov radiation has ever been observed.

In a previous paper [14] we described initial efforts to measure the coherent radio-frequency (RF) emission from electron bunches interacting in a solid dielectric target of 360 kg of silica sand. That study, done with low-energy electrons (15 MeV), demonstrated the presence of coherent radiation in the form of extremely short and intense microwave pulses detectable over a wide frequency range. These results, while useful for understanding the coherent RF emission processes from relativistic charged particles, could not directly test the development of a shower charge excess, as Askaryan predicted. Also, because the particles were charged, passage of the beam through any interface induced strong RF transition radiation (TR), which obscured the presence of Cherenkov radiation (CR).

We have previously reported on these measurements made at the Stanford Linear Accelerator Center (SLAC) [15]. We used high-energy photons, rather than low-energy electrons, has enabled us to clearly observe microwave Cherenkov radiation from the Askaryan effect. In this report we add a few plots: the shower profile measured at C-band, the shock-wave behavior and the intensity relative to the Cherenkov angle.

II EXPERIMENTAL SETUP

A silica sand target and antennas were placed in a gamma-ray beamline in the Final Focus Test Beam facility at SLAC in August 2000. The apparatus was placed 30 m downstream of aluminum bremsstrahlung radiators that produced a high-energy photon beam from 28.5 GeV electrons. Beyond the radiators, the electron beam was bent down, and dumped 15 m beyond our target. Typical beam currents during the experiment were $(0.2-1.0)\times 10^{10}$ electrons per bunch. The two radiators could be used either separately or in tandem, thereby providing 0%, 1%, 2.7% or 3.7% of a radiation length. Thus the effective shower energy induced by the photons could be varied from $(0.06-1.1)\times 10^{19}$ eV per bunch. The size of the photon bunch at the entrance of the silica sand target was less than several mm in all directions and is negligible compared to the instantaneous shower dimensions.

The target was a large container built largely from non-conductive materials such as wood and plastic which we filled with 3200 kg of dry silica sand. As shown in Fig. 1, the sand target was rectangular in cross section perpendicular to the beam axis, but the vertical faces on both sides were angled to facilitate transmission of radiation arriving at the Cherenkov angle (about 51° in silica sand at microwave frequencies). We avoided making sides parallel to the beam since the CR would

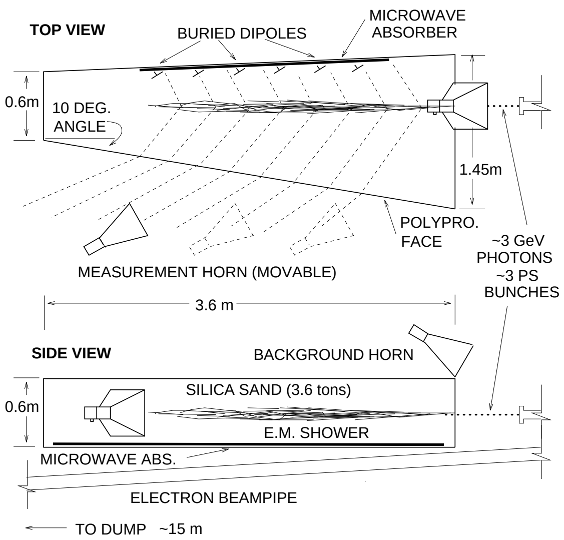

FIGURE 1. Sectional views of the target geometry.

then suffer total internal reflection at the interface. Both internal (buried) half-wave dipoles and external antennas were used for the pulse measurements. The external antennas were pyramidal "standard gain" microwave horns (1.7–2.6 GHz or 4.4–5.6 GHz). A 0.5 in. low-microwave-loss polypropylene was used for the face viewed by the external antennas.

Details of the trigger system, data acquisition, and polarization and power measurements were similar to those used in our previous experiment [14]. Briefly, time-domain sampling of the antenna voltages using high-bandwidth oscilloscopes allowed us to make direct measurements of the electric field of the pulses as a function of time, with time resolutions of 100 ps (0.2–3 GHz) and 10 ps (4–6 GHz). Because of the strength of the signals no amplification was required. Microwave absorber material was placed wherever possible to minimize reflections, and the geometry was chosen so that, where reflections could not be eliminated, they would arrive well after the expected main pulse envelope. The incident electron beam current was measured using a beam current transformer.

Because the accelerator itself uses S-band (2.9 GHz) RF for the beam generation, we took particular care to measure the background levels of RF with the electron beam on, but no photon radiators in place. A weak background RF pulse with a few mV r.m.s. in coincidence with the beam proved completely negligible compared to the signal pulses detected with the photon beam on target, typically 10-100 V peak-to-peak. In addition, we used a second S-band horn to monitor any incoming radiation (see fig. 1). These and numerous other tests such as the lack of effect from moving absorbers eliminated the possibility that stray linac RF or other RF associated with the electron beam contributed to our measurements.

We checked the static magnetic field strength in the vicinity of our sand target and found it to be comparable to ambient geomagnetic levels. This is important since stray fields present in the accelerator vault could have induced significant charge separation in showers within our target and led to other radiation mechanisms. In 0.5 Gauss, the electron gyroradius for the bulk of the shower is ≥ 1 km, implying charge separations of ≤ 1 cm over the length of a shower, well below the ~ 4 cm Molière radius.

III RESULTS

A Time & shower profiles

The inset to fig. 2 shows a typical pulse profile measured with one of the S-band horns aimed near shower maximum. Given that the bandwidth of the horn is 900 MHz, the ~ 1 ns pulse width indicates a bandwidth-limited signal. This behavior is seen at all frequencies observed, with the best upper limit to the intrinsic pulse width, based on the 4.4–5.6 GHz data, being less than 500 ps.

Fig. 2 also shows a set of measured peak field strengths for pulses taken at different points along the shower. Both the S-band and C-band horns were translated parallel to the shower axis, maintaining the same angle (matched to the refracted Cherenkov angle) at each point. The values are plotted at a shower position corresponding to the center of the antenna beam pattern, refracted onto the shower. The half-power beamwidth of the horn is about $\pm 10°$; thus the antenna would respond to any isotropic shower radiation over a range of $\pm 20 - 25$ cm around the plotted positions. The CR radiation pattern is expected to have a total beamwidth less than several degrees [3,16], much smaller than the antenna beam pattern.

The plotted curve shows the expected profile of the total number of particles in the shower, based on the KNG [17] approximation. Here the axes have been chosen to provide an approximate overlay of the field strengths onto the shower profile. Clearly the pulse strengths are highly correlated to the particle number. Since the excess charge is also expected to closely follow the shower profile, this result is consistent with Askaryan's hypothesis.

Since CR propagates as a conical bow shock from the shower core, the pulse wavefront traverses any line parallel to the shower axis at the speed of the shower ($\simeq c$) rather than the local group velocity c/n. Using our buried dipole array we have confirmed such behavior. The arrival times of the pulse at each dipole are shown in fig. 3 and imply a radiative bow shock at $v/c = 1.0 \pm 0.1$, inconsistent with the measured group velocity ($0.6\ c$) in the target.

Additional observations with an external S-band horn at the top interface of the sand show evidence for total internal reflection. We observed ~ 34 dB attenuation of the pulse transmitted through the surface, which is approximately parallel to the shower axis. This latter behavior is characteristic of CR, since the Cherenkov angle is the complement of the angle of total internal reflection to vacuum.

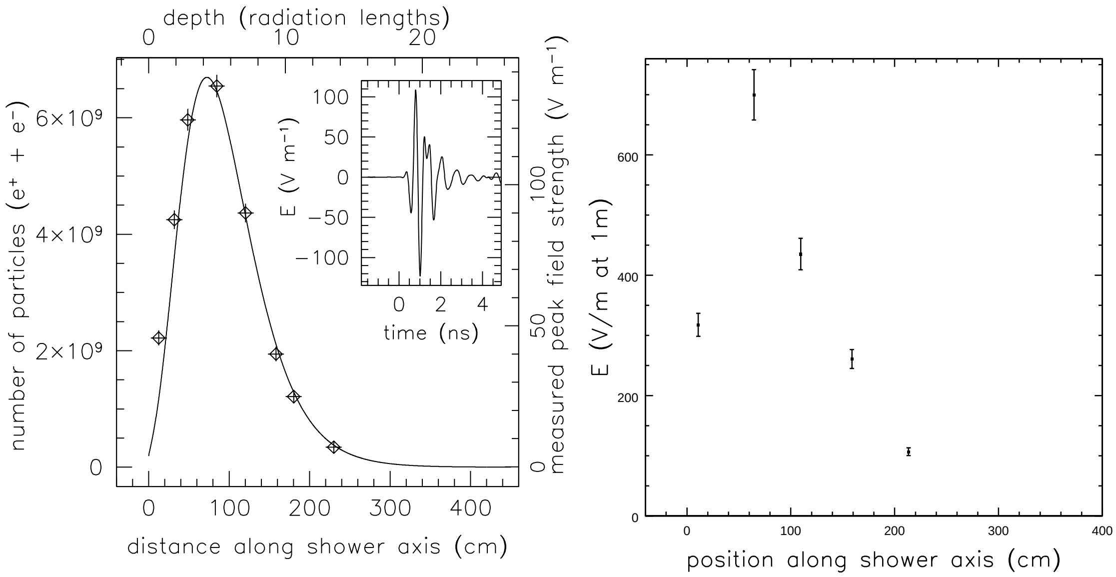

FIGURE 2. left:Expected shower profile (solid), with measured peak field strengths (diamonds) plotted normalized to the peak. Inset: typical pulse time profile. right: Profile using the C-band data.

Pulse polarization was measured with an S-band horn directed at a shower position 0.5 m past the shower maximum. Field intensities were measured with the horn rotated at angles 0, 45, 90 and 135 degrees from horizontal. Fig. 3 shows the pulse profile for both the 0° and 90° (cross-polarized) orientations of the horn. Fig. 3 also shows the degree of linear polarization and the angle of the plane of polarization, respectively. The results are completely consistent with Cherenkov radiation from a source along the shower axis. Since the position was downstream of shower maximum, late reflections from the upper surface of the sand enter the pulse profile, resulting in a loss of polarization beyond ~ 2 ns.

B Coherence

Fig. 4 shows a sequence of pulse field strengths for the external S-band horn versus the total shower energy, which was varied both by changing the beam current and the thickness of the radiators. The curve is a least-squares fit to the data, of the form $|\mathbf{E}| \propto (W_T)^\alpha$ where $|\mathbf{E}|$ is the electric field strength and W_T is the total shower energy. The fit yields $\alpha = 0.96 \pm 0.05$, consistent with complete coherence of the radiation, implying the characteristic quadratic rise in the corresponding pulse power with shower energy.

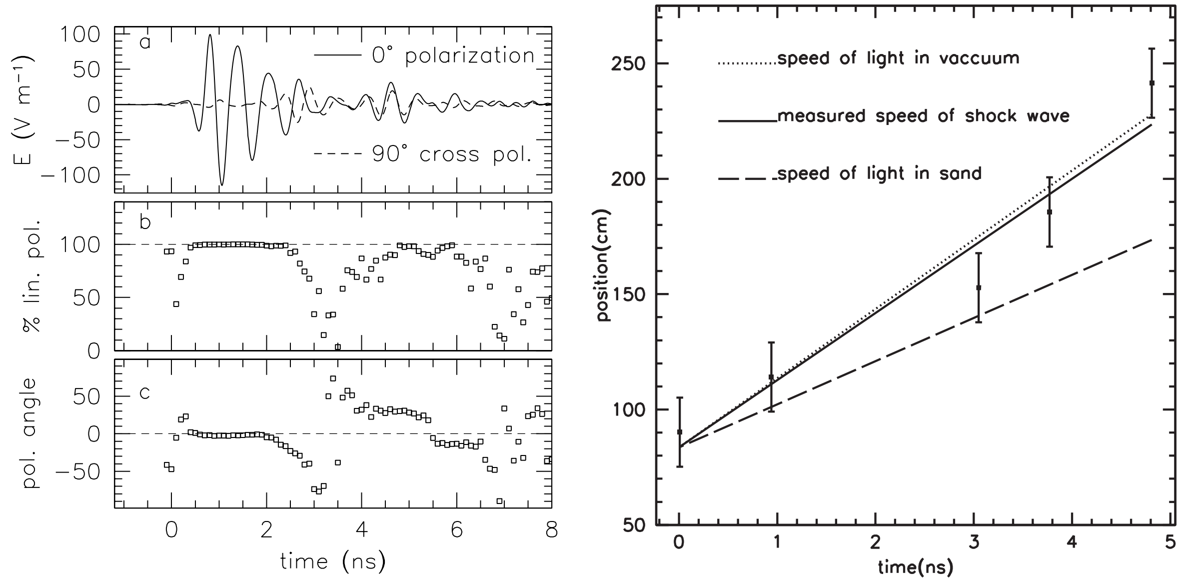

FIGURE 3. left:Polarization analysis of the pulses recorded by the S-band horns. (a) the measured field strength of the pulse, (b) the fractional linear polarization, (c) the angle of the plane of polarization, where 0° is horizontal. right: Electric field normalized to 1 m distance relative to Cherenkov angle–after accounting for refraction at interface.

C Angular dependence

The shape of the target (see fig. 1) was designed to facilitate the measurement of the shower profile. Because the antennas were so close to the shower, angular measurements could not be made by simply rotating the horn–which would then point to a different part of the shower. Instead, we took a series of measurements for which the horn axis was rotated off of the expected direction of the Cherenkov radiation from shower max (after being refracted by the sand-air interface). This required moving the horn longitudinally. As a result the field measurements needed to be corrected for differerent distances from shower max (a linear correction) as well as a small (<10%) correctoin for the changing integral track length in the antenna aperture. The angular response is shown in fig. 4. Uncertainties are due primarily to the precision of antenna positioning and interpretation of the pulse shape. The data show a peak at the expected Cherenkov angle with a width roughly consistent with the antenna response, indicating that the width of the Cherenkov "beam" is much narrower than the antenna's beam, as expected.

D Spectral dependence and absolute intensity

Fig. 4 shows the measured spectral dependence of the radiation. superimposed on a curve based on a parameterization of Monte Carlo results [3,18] which we have corrected for the differences between ice and sand and for the fact that the limited antenna apertures are only sensitive to about half of the total field strength. A parameterization is also available [19] that accounts for various near-field effects but is not straightforward to apply to our case. The error bars are conservative estimates of effects due to uncertainties in surveying, interpretation of pulse shapes, antenna response, and beam intensity. Note that Fig. 4 compares absolute field strength measurements to the predictions and the agreement is very good.

IV DISCUSSION

We have demonstrated that the radiation we have observed is coherent and 100% linearly polarized in the plane containing the antenna and shower axis and is emitted as a shock wave at the Cherenkov angle in sand. The radiation is pulsed with time durations much shorter than the inverse bandwidth of our antennas. The strength of the pulse is strongly correlated to the size (in particle number) of the shower region that appears to produce it. All of these characteristics are consistent with the hypothesis that we have observed coherent Cherenkov radiation. Because of the strong correlation with the shower profile and the physical constraint that a shower with no net excess charge cannot radiate, we conclude that excess charge production along the shower is the source of the CR observed. These conclusions are strengthened by the agreement of the absolute field strengths with predictions.

Our observations are inconsistent with radiation from geomagnetic charge separation as observed in extensive air showers. The most striking evidence is that the plane of polarization is clearly aligned with the shower axis rather than the local geomagnetic dip angle (62°). Given the approximate east-west orientation of the shower axis, radiation from geomagnetic charge separation would have produced an electric field polarization with significant components orthogonal to what we have observed.

We note that in all cases our measurements are likely to be made in near-field conditions, and we have not attempted to correct for these effects. Recent studies [19,18] have begun to treat these issues, but are not straightforward to apply in our case. In any case, near field effects should generally *decrease* the measured field strengths relative to far field measurements.

The total energy of our cascades is as high as 10^{19} eV, but these showers consist of the superposition of many lower-energy showers. Higher-energy effects [4] would have elongated the shower and tended to increase the total tracklength of the shower, at the expense of a lower instantaneous particle number density. The net effect is that the total radiated power is expected to be approximately conserved, but the angular distribution would sharpen significantly. Scaling of our results to high energy showers should consider corrections for these effects, which are likely to increase the peak field strengths in far-field measurements.

Extrapolations to determine the energy threshold of existing experiments are possible, after correcting for the differences in material properties. For Antarctic ice

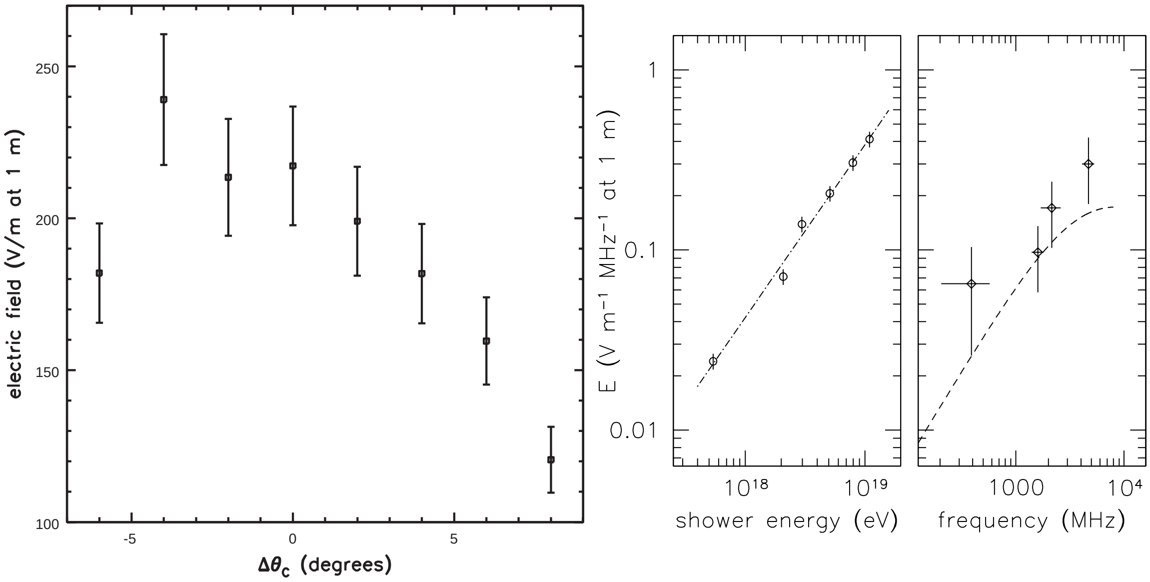

FIGURE 4. (a) Measured coherence of pulse electric field vs. shower energy, at 2.1 GHz. The curve is a least-squares fit. (b) Spectral dependence of the measured pulse field strengths. The horizontal bars indicate the antenna bandwidth, and the vertical bars the uncertainties. The curve is based on a theoretical prediction described in the text.

experiments, the use of the existing simulations [3–5] appears completely justified. For experiments observing the lunar regolith [7–9], silica sand shares many similarities with the lunar surface material, and the expected cascade energy threshold is $\sim 2 \times 10^{19}$ eV. Note that showers from a single high energy particle would be longer than the superposition of low-energy showers used in this study and while the total radiated power would be approximately conserved, the far-field angular distribution would sharpen and lead to possibly even lower thresholds.

In combination with our previous measurements of coherent TR [14], these results have established a firm experimental basis for radio-frequency detection of high energy cascades in solid media, either through interaction within a dielectric (for CR), or via passage through interfaces (for TR). Above cascade energies of $\sim 10^{16}$ eV, these processes become dominant over optical Cherenkov or fluorescence emission in the number of quanta produced [2]. Thus experiments designed to exploit this effect in the detection of ultra-high energy particles can now be pursued with even greater confidence.

V ACKNOWLEDGMENTS

We thank D. Besson, R. Rose, L. Skjerve, and M. Spencer for the loan or construction of several antennas. We thank the members of the SLAC accelerator and EF departments for invaluable assistance before, during and after the run. This research was supported in part by by DOE contract DE-FG03-91ER40662 at UCLA and the Sloan Foundation. It has been performed in part at the Jet Propulsion Laboratory, Caltech, under contract with NASA. SLAC is supported by the DOE, with work performed under contract DE-AC03-76SF00515. Argonne is supported by DOE contract W-31-109-ENG-38.

REFERENCES

1. G. Askaryan, Soviet Physics JETP **14**, 441 (1962); G. Askaryan, Soviet Physics JETP **21**, 658 (1965).
2. M. A. Markov and I. M. Zheleznykh, Nucl. Instr. Meth. A248, 242, (1986).
3. E. Zas, F. Halzen, and T. Stanev, Phys. Rev. D **45**, 362 (1992).
4. J. Alvarez–Muñiz and E. Zas, Phys. Lett. B, **411**, 218 (1997); J. Alvarez–Muñiz and E. Zas, Phys.Lett. B, **434**, 396, (1998); J. Alvarez–Muñiz, R.A. Vázquez, and E. Zas, Phys.Rev. D61 (2000), 023001.
5. G. M. Frichter, J. P. Ralston, and D. W. McKay, Phys. Rev. D. **53**, 1684 (1996).
6. D. Besson *et al.*, Proc. 26th. Intl. Cosmic Ray Conf., v. 2, 467 (1999).
7. I. Zheleznykh, Proc. 13th Intl. Conf. on Neutrino Physics and Astrophysics, World Scientific, Boston, ed. J. Schreps, p. 528 (1988); R. Dagkesamanskii, and I. Zheleznykh, JETP Lett., **50** 259 (1989).
8. T. H. Hankins, R. D. Ekers, and J. D. O'Sullivan, MNRAS **283**, 1027 (1996).
9. P. W. Gorham, K. M. Liewer, and C. J. Naudet, Proc. 26th Intl. Cosmic Ray Conf., v 2, 479, (1999); astro-ph/9906504.
10. J. V. Jelley, et al., Nuovo Cimento 46, 649, (1966).
11. D. Fegan and N. A. Porter, Nature 217, 440, (1968).
12. F. D. Kahn, and I. Lerche, Proc. Roy. Soc. A 289, 206 (1966).
13. H. R. Allan, in *Prog. in Elem. Part. & Cosmic Ray Phys.* 10, ed. J. G. Wilson & S. G. Wouthuysen (North-Holland: Amsterdam), 171, (1971).
14. P. W. Gorham, D. P. Saltzberg, P. Schoessow, *et al.*, Phys. Rev. E, **62**, 8590 (2000).
15. D. Saltzberg, P. Gorham, D. Walz *et al.*, Phys. Rev. Lett., in press, hep-ex/0011001 (2001). +
16. T. Takahashi, *et al.*, Phys. Rev. E **50**, 4041 (1994).
17. K. Kamata and J. Nishimura, 1958, Suppl. Progr. Theoret. Phys. 6, 93; K. Greisen., 1965, Prog. Cosmic Ray Phys. vol. III, J. Wilson ed., (No. Holland: Amsterdam) 1.
18. J. Alvarez–Muñiz, R.A. Vázquez, and E. Zas, Phys. Rev. D62 (2000), 063001.
19. R. V. Buniy and J. P. Ralston, astro-ph/003408 (2000).